Spin- and Parity-Resolved Level Densities from the Fine Structure of Giant Resonances

Y. Kalmykov,[1] C. Özen,[2] K. Langanke,[1,2] G. Martínez-Pinedo,[2] P. von Neumann-Cosel,[1,*] and A. Richter[1]

[1]*Institut für Kernphysik, Technische Universität Darmstadt, D-64289 Darmstadt, Germany*

[2]*Gesellschaft für Schwerionenforschung, D-64291 Darmstadt, Germany*

(Received 21 June 2007; published 16 November 2007)

Level densities of $J^\pi = 2^+$ and 2^- states extracted from high-resolution studies of $E2$ and $M2$ giant resonances in ^{58}Ni and ^{90}Zr are used to test recent predictions of a possible parity dependence. The experimental results are compared to a combinatorial approach based on the Hartree-Fock-Bogoliubov model and to shell-model Monte Carlo calculations including both spin and parity projection. No parity dependence is observed experimentally, which is in agreement for ^{90}Zr but in contrast with the model predictions for ^{58}Ni.

DOI: 10.1103/PhysRevLett.99.202502 PACS numbers: 21.10.Ma, 21.60.Cs, 24.30.Cz, 27.40.+z

Level densities represent an important test of nuclear structure models. They also play a crucial role in the calculation of reaction cross sections, of particular importance in astrophysical applications [1]. Total level densities are often described [1,2] assuming a noninteracting Fermi gas model corrected for the effects of pairing of nucleons by an empirical shift in excitation energy, the so-called backshifted Fermi gas model (BSFG). Implicit to such models is the assumption of levels with positive and negative parity being equally probable. However, recent microscopic calculations in the shell-model Monte Carlo (SMMC) approach cast some doubts on this issue, predicting a significant parity dependence of total level densities for certain pf shell nuclei up to excitation energies as high as 20 MeV [3]. This is also found for individual spin values using a quantum Monte Carlo approach [4]. A global study using a simplified quasiparticle model confirms this result over wider shell and mass ranges [5]. A Hartree-Fock-Bogoliubov (HFB) plus combinatorial model including collective effects due to vibrations and rotation also predicts this effect, but on top of it large fluctuations of the level densities [6].

Total level density ratios have been extracted by counting levels of each parity in experimental spectra [7] but require complete data sets and are therefore restricted to low energies only. Here we address this question with spin- and parity-resolved level densities obtained by a fluctuation analysis of high-resolution data on the fine structure of electric and magnetic giant resonances. In particular we show the direct comparison of $J^\pi = 2^+$ and 2^- level densities in the same nuclei and for the same excitation energies allowing for a direct experimental test of a possible parity dependence. One such test has already been reported [8] at energies close to the particle emission threshold utilizing s- and p-wave proton resonance capture. No parity dependence was found comparing $1/2^\pm$ and $3/2^\pm$ level densities in ^{45}Sc. The present findings are compared to the predictions of Ref. [6] and—for the first time—to SMMC calculations resolved in spin and parity.

The equilibration of levels with different parity is governed by two distinct energy scales associated with pair breaking on one side and the gap between opposite-parity states near the Fermi surface on the other side. The former is typically of order 5–6 MeV for intermediate-mass even-even nuclei. The latter, however, strongly depends on nuclear structure. Here we select two cases, ^{58}Ni and ^{90}Zr, with quite distinct features of the two energy scales. For ^{58}Ni the Fermi surface is in the middle of the pf shell and a rather large energy gap has to be overcome to create states with negative parity. In contrast, ^{90}Zr has a closed proton pf shell within the independent particle model. Hence, any odd number of proton excitations across the $pf - g_{9/2}$ shell gap, which is of order 3 MeV, leads to negative-parity states.

The extraction of $J^\pi = 2^\pm$ level densities is based on high-resolution studies of $E2$ and $M2$ giant resonances in ^{58}Ni and ^{90}Zr with inelastic proton and electron scattering, respectively. In the proton scattering experiments [9,10] angles near the maximum of $\Delta L = 2$ transitions were chosen to selectively excite 2^+ states in the energy region of the isoscalar giant quadrupole resonance. Electron scattering was performed in kinematics where the $M2$ resonance was enhanced [11,12]. Figure 1 shows examples of the ^{58}Ni(p, p') and ^{58}Ni(e, e') spectra.

A direct comparison of the $2^\pm$ level densities is possible at excitation energies $E_x = 7$–15 MeV in ^{58}Ni and 7–12 MeV in ^{90}Zr, where both giant resonances overlap. In these energy regions the mean level width $\langle\Gamma\rangle$ is smaller than the mean level spacing $\langle D\rangle$, and both are smaller than the experimental energy resolution ΔE [13]. Thus, fluctuations in the cross section result from the high density of unresolved states due to their incoherent overlap. In this regime, level spacings can be determined by means of a fluctuation analysis [14]. Examples of the application to high-resolution spectra are described, e.g., in Refs. [12,15–17]. The measured spectrum is convoluted with a Gaussian whose width is large compared to ΔE. To take into account finite statistics the spectrum is also folded with a Gaussian with a width smaller than ΔE. Dividing the latter by the former spectrum leads to a stationary spectrum $d(E_x)$ distributed around $\langle d(E_x)\rangle = 1$. The autocorrelation function

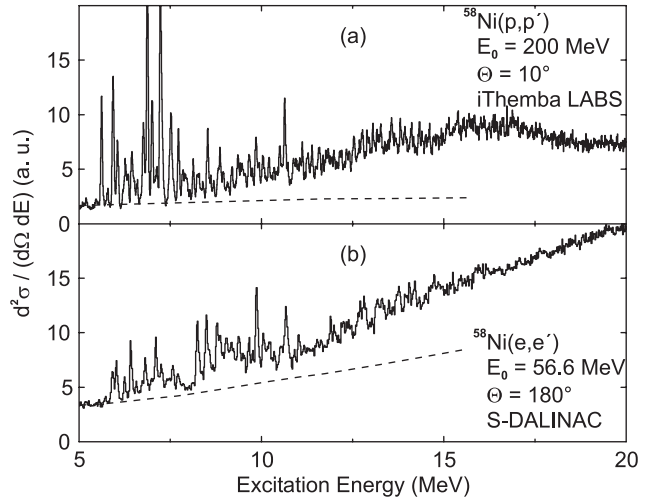

FIG. 1. Spectrum of the (a) ^{58}Ni(p, p') reaction at $E_0 =$ 200 MeV and $\Theta = 10°$ [9], and (b) ^{58}Ni(e, e') reaction at $E_0 =$ 56.6 MeV and $\Theta = 180°$ [11]. Backgrounds (dashed lines) are determined by the wavelet analysis described in the text.

$$C(\epsilon) = \langle d(E_x) d(E_x + \epsilon) \rangle \tag{1}$$

is a measure of the spectral fluctuations with respect to a local mean value. Here, the brackets indicate averaging over the interval for which the analysis is performed, and ϵ is the energy increment. The experimental autocorrelation function, Eq. (1), at $\epsilon = 0$ can be connected to $\langle D \rangle$ via the theoretical expression derived in [14]:

$$C(\epsilon) = 1 + \frac{\alpha \langle D \rangle}{2\Delta E \sqrt{\pi}} f(\epsilon, \Delta E). \tag{2}$$

The function $f(\epsilon, \Delta E)$, given, e.g., in [15], is normalized such that $f(\epsilon = 0) = 1$. Equation (2) is based on the assumption that the level spacing and intensity distributions are Wigner- and Porter-Thomas-like, respectively, from random matrix theory [18]. The value α is a sum of the normalized variances of the spacing and transition width distributions, which is known exactly for a single class of states. Thus, high selectivity of the reaction exciting levels of a certain J^π is beneficial for a model-independent analysis. Another requirement obvious from Eq. (2) is high-resolution data, since the autocorrelation signal is damped with increasing ΔE.

A large systematic error in the determination of $\langle D \rangle$, which is the inverse of the level density, arises from insufficient knowledge of nonresonant background contributions in the spectra. To determine this background, the fluctuation analysis has been extended and combined with a wavelet analysis [19]. By folding the original spectrum $\sigma(E)$ with a wavelet function Ψ, wavelet coefficients

$$C(E_x, \delta E) = \frac{1}{\sqrt{\delta E}} \int \sigma(E) \Psi\left(\frac{E_x - E}{\delta E}\right) dE \tag{3}$$

are obtained. The parameters (excitation energy E_x and scale δE) are varied in discrete steps: $\delta E = 2^j$; $E_x = k\delta E$; $j, k = 1, 2, 3 \ldots$, which allows to reassemble the original signal from the wavelet coefficients. The present application utilizes the property of vanishing moments

$$\int E^n \Psi(E) dE = 0, \qquad n = 0, 1 \ldots m \tag{4}$$

of many wavelet functions. Then, any nonresonant background in the spectrum, whether of physical or experimental nature, does not contribute to the wavelet coefficients if it can be approximated by a polynomial function of order m. This allows for a nearly model-independent background determination applied earlier to the high-resolution ^{90}Zr(^{3}He, t)^{90}Nb data in [20] for the first time. Application of this method to the spectra displayed in Fig. 1 leads to backgrounds indicated by the dashed lines.

Experimental densities for $J = 2^+$ and 2^- levels are shown in Figs. 2 and 3 for ^{58}Ni and ^{90}Zr, respectively. Principal accuracy limits of a fluctuation analysis as described above are discussed in [17]. The uncertainties shown take into account the influence of the widths of the smoothing functions and the chosen interval length as well as finite-range-of-data errors.

We start the comparison of our data (solid circles) to the model predictions with the BSFG approach using the parametrization of Ref. [1] shown by solid lines. As the BSFG provides no parity information, the level densities are divided by a factor of 2. Both absolute values and energy dependence are well described in all cases.

Spin- and parity-projected level densities from the HFB model [6] available in a table format for fixed excitation energies [21] are shown as open triangles in Figs. 2 and 3. In case of ^{90}Zr, the HFB results are systematically somewhat too low, while in ^{58}Ni agreement is achieved at higher excitation energies but the model overpredicts (underpre-

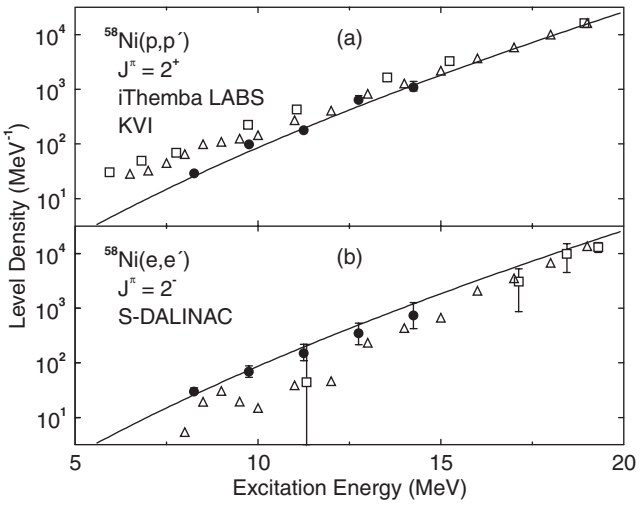

FIG. 2. Experimental (solid circles) level densities of (a) 2^+ and (b) 2^- states in ^{58}Ni compared to BSFG (solid lines), HFB (open triangles), and SMMC (open squares) predictions.

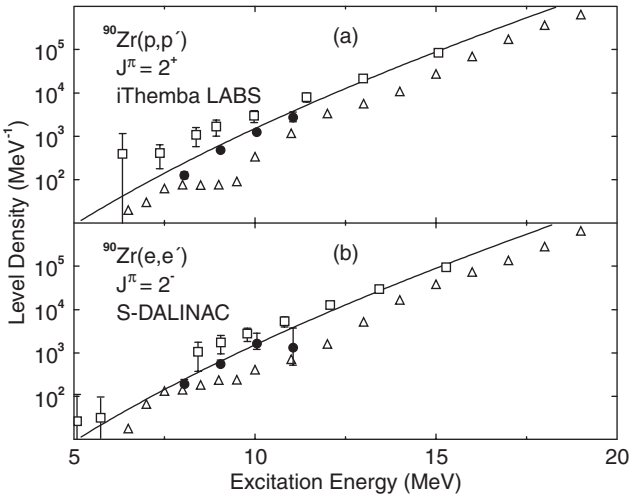

FIG. 3. Same as Fig. 2, but for ^{90}Zr.

dicts) the number of $2^+(2^-)$ states toward lower excitation energies. An interesting feature of the HFB results, discussed in more detail below, is strong oscillations as a function of excitation energy around a local mean value whose energy dependence follows more or less the expected exponential growth.

Thirdly, we compare the data to results obtained with the SMMC approach. The method [22,23] has proven to be a powerful tool for the computation of level densities [24,25] and their dependence on parity [3,26] and angular momentum [27]. Here, combined spin and parity projection are applied. In the SMMC approach the excitation energy E_J^π for a given J^π value can be evaluated as the expectation value of the many-body Hamiltonian H in a heat bath with inverse temperature β. The associated level density ρ_J^π is determined from

$$E_J^\pi(\beta) = \frac{\mathrm{Tr}_{J,\pi}[He^{-\beta H}]}{Z_J^\pi(\beta)} = \frac{\int dE' e^{-\beta E'} E' \rho_J^\pi(E')}{Z_J^\pi(\beta)}, \quad (5)$$

where $Z_J^\pi(\beta) \equiv \mathrm{Tr}_{J,\pi} e^{-\beta H}$ is the partition function of many-body states with fixed J^π. In the second step we have related E_J^π to the level densities of states with quantum numbers J^π. The level density can then be obtained by employing an inverse Laplace transform in the saddle-point approximation

$$\rho_J^\pi(E) = \frac{e^{\beta E_J^\pi + \ln Z_J^\pi(\beta)}}{\sqrt{-2\pi \frac{dE_J^\pi(\beta)}{d\beta}}}. \quad (6)$$

The calculations have been performed in the complete $fp - gds$ model space with 50 valence orbitals for both protons and neutrons and a pairing-plus-quadrupole-type residual interaction. Single-particle energies and interaction parameters have been adopted from previous studies [26,28] and have been validated against low-energy properties of $A \sim 64$ nuclei [29].

The SMMC results are plotted as squares in Figs. 2 and 3. Clearly, they are of different quality for ^{58}Ni and ^{90}Zr. In ^{90}Zr, data are overestimated for both parities but approach the BSFG result at higher E_x. In ^{58}Ni the SMMC and HFB results are quite close, overpredicting the number of 2^+ states and underpredicting 2^- states.

Let us now address the question of a possible parity dependence. The ratios of 2^- and 2^+ level densities in ^{58}Ni and ^{90}Zr are presented in Fig. 4. For better comparison the model results are shown as continuous lines. For the HFB results these are determined assuming an exponential behavior between the available points. Since for a given value of β the $E_J^\pi(\beta)$ values are different for positive and negative parities, the SMMC results have been fitted with a BSFG formula.

Importantly, in both nuclei the experimental data are consistent within error bars with an equal number of states for both parities. This is in noticeable contrast to the predictions of the microscopic models. The SMMC result for ^{58}Ni shows a slow increase of the ρ_-/ρ_+ ratio in the measured energy range similar to previous studies of other mid-pf shell nuclei [3,26] and $\rho_-/\rho_+ \simeq 1$ is reached only around 20 MeV. A hint on the origin of this failure may rest in the size of the model spaces. While the pf-gds model space is probably sufficient for the 2^+ states, it underestimates the negative-parity level densities due to the neglect of core excitations from sd shell orbitals close to the Fermi surface. On the other hand, quantum Monte Carlo calculations [4] for the isotone ^{56}Fe allowing for an even larger $sd - pf - gds$ valence space still predict a significant suppression of ρ_- in the energy range investigated here. In ^{90}Zr equilibration of levels with positive and negative parity in the SMMC calculation is already reached at low excitation energies due to the small gap for

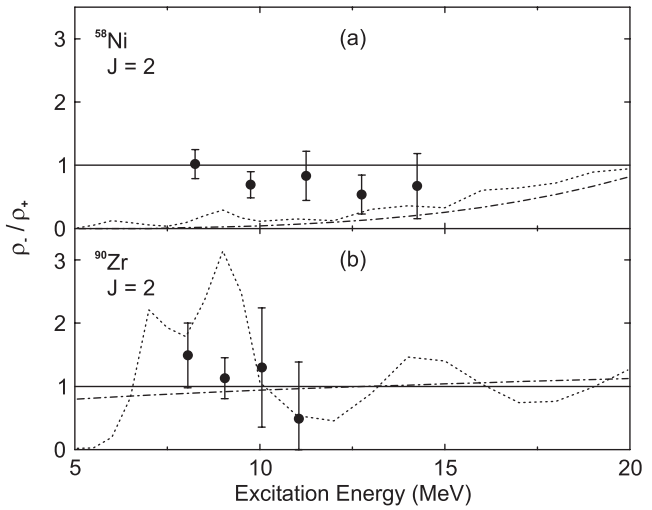

FIG. 4. Experimental ratio (solid circles) of negative- to positive-parity level densities of $J = 2$ states in (a) ^{58}Ni and (b) in ^{90}Zr compared to BSFG (solid lines), HFB (dotted lines), and SMMC (dash-dotted lines) predictions.

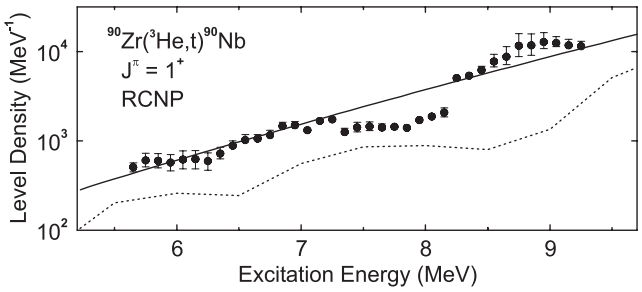

FIG. 5. Comparison of experimental level densities for 1^+ states in ^{90}Nb (solid circles) with predictions of the BSFG (solid line) and the HFB (dashed line) approaches.

the negative-parity excitations. The ratios predicted by HFB disclose pronounced fluctuations in the case of ^{90}Zr, but the oscillations are damped with increasing excitation energy and are compatible with a mean value of one. For ^{58}Ni, a behavior similar to the SMMC results is found.

Finally, we briefly address the question of level density fluctuations. Figure 5 shows level densities for 1^+ states in ^{90}Nb, extending the results presented in [20]. The analysis has been carried out for a large number of partially overlapping energy intervals and systematic errors have been treated in a consistent way. Indeed, the data exhibit significant oscillations around an exponential growth inherent to the BSFG model (solid line) describing the average increase with excitation energy. While the overall scale of the HFB result is too low, the fluctuations with excitation energy resemble the experimental results qualitatively. One might speculate that the fluctuations are a signature of pair breaking leading to a sudden increase of ρ at $E_x \simeq$ 6.5 and 8.5 MeV (for a similar observation in total level densities, see [30]). However, a systematic study of this effect in other nuclei and for different J^{π} values is needed before one can draw definite conclusions.

To summarize, we have extracted level densities of 2^+ and 2^- states from high-resolution studies of $E2$ and $M2$ giant resonances in ^{58}Ni and ^{90}Zr. The approach is based on a fluctuation analysis combined with a new method for background determination utilizing a wavelet analysis. In the investigated excitation energy range (up to 15 MeV in ^{58}Ni and up to 12 MeV in ^{90}Zr) we do not find any sign of a parity dependence in contrast to microscopic predictions [3,5,6] for ^{58}Ni. The SMMC results suggest that the problem lies in a still insufficient model space for the negative-parity states. A high-resolution study of the GT resonance in ^{90}Nb suggests strong fluctuations of the 1^+ level density up to unexpectedly high excitation energies, which might be due to pair breaking.

We are indebted to Y. Alhassid, S. Goriely, P. Leboeuf, and G. E. Mitchell for valuable discussions. This work was supported by the DFG under Contracts No. SFB 634 and No. NE 679/2-2. Computational resources were provided by the NCCS at ORNL, which is managed by UT-Battelle, LLC, for the U.S. DOE under Contract No. DE-AC05-00OR22725.

*vnc@ikp.tu-darmstadt.de

[1] T. Rauscher, F.-K. Thielemann, and K.-L. Kratz, Phys. Rev. C **56**, 1613 (1997).
[2] T. von Egidy and D. Bucurescu, Phys. Rev. C **72**, 044311 (2005); **73**, 049901 (2006).
[3] H. Nakada and Y. Alhassid, Phys. Rev. Lett. **79**, 2939 (1997); Y. Alhassid *et al.*, Phys. Rev. Lett. **84**, 4313 (2000).
[4] K. Van Houcke *et al.*, arXiv:nucl-th/0702041.
[5] D. Mocelj *et al.*, Phys. Rev. C **75**, 045805 (2007).
[6] S. Hilaire and S. Goriely, Nucl. Phys. A **779**, 63 (2006).
[7] S. I. Al-Quraishi *et al.*, Phys. Rev. C **67**, 015803 (2003).
[8] S. J. Lokitz, G. E. Mitchell, and J. F. Shriner, Jr., Phys. Lett. B **599**, 223 (2004).
[9] A. Shevchenko *et al.*, Phys. Rev. Lett. **93**, 122501 (2004); A. Shevchenko, Doctoral thesis, D17, Technische Universität Darmstadt, 2005.
[10] F. Hofmann *et al.*, Phys. Lett. B **612**, 165 (2005).
[11] B. Reitz *et al.*, Phys. Lett. B **532**, 179 (2002); B. Reitz, Doctoral thesis, D17, Technische Universität Darmstadt, 2000.
[12] P. von Neumann-Cosel *et al.*, Phys. Rev. Lett. **82**, 1105 (1999).
[13] The systematics of Γ extracted from Ericson fluctuation data suggest $\langle\Gamma\rangle \simeq 1$ keV in ^{58}Ni at 15 MeV [K. A. Eberhard and A. Richter, *Proc. Int. Conf. on Statistical Properties of Nuclei*, edited by J. B. Garg (Plenum Press, New York, 1972), p. 139] and consequently $\langle\Gamma\rangle/\langle D\rangle \approx 1$ for the present case. However, this is a conservative estimate since the particle emission thresholds are high in ^{58}Ni.
[14] P. G. Hansen, B. Jonson, and A. Richter, Nucl. Phys. A **518**, 13 (1990).
[15] S. Müller *et al.*, Phys. Lett. B **113**, 362 (1982).
[16] J. Enders *et al.*, Phys. Rev. Lett. **79**, 2010 (1997).
[17] T. Døssing *et al.*, Phys. Rep. **268**, 1 (1996).
[18] T. Guhr, A. Müller-Groeling, and H. A. Weidenmüller, Phys. Rep. **299**, 189 (1998).
[19] *Wavelets in Physics*, edited by J. C. van den Berg (Cambridge University Press, Cambridge, England, 1999).
[20] Y. Kalmykov *et al.*, Phys. Rev. Lett. **96**, 012502 (2006).
[21] http://www-astro.ulb.ac.be/html/nld_comb.html.
[22] S. E. Koonin, D. J. Dean, and K. Langanke, Phys. Rep. **278**, 1 (1997).
[23] C. W. Johnson *et al.*, Phys. Rev. Lett. **69**, 3157 (1992).
[24] W. E. Ormand, Phys. Rev. C **56**, R1678 (1997).
[25] K. Langanke, Phys. Lett. B **438**, 235 (1998).
[26] C. Özen *et al.*, Phys. Rev. C **75**, 064307 (2007).
[27] Y. Alhassid, S. Liu, and H. Nakada, Phys. Rev. Lett. **99**, 162504 (2007).
[28] K. Langanke, D. J. Dean, and W. Nazarewicz, Nucl. Phys. A **728**, 109 (2003).
[29] D. J. Dean (private communication).
[30] E. Melby *et al.*, Phys. Rev. Lett. **83**, 3150 (1999).